Universität Regensburg
Mathematik

Phase-field approaches to structural topology optimization

Luise Blank, Harald Garcke, Lavinia Sarbu, Tarin Srisupattarawanit, Vanessa Styles and Axel Voigt

Phase-field approaches to structural topology optimization

Luise Blank, Harald Garcke, Lavinia Sarbu, Tarin Srisupattarawanit, Vanessa Styles and Axel Voigt

Abstract. The mean compliance minimization in structural topology optimization is solved with the help of a phase field approach. Two steepest descent approaches based on L^2- and $H^{-1}-$gradient flow dynamics are discussed. The resulting flows are given by Allen-Cahn and Cahn-Hilliard type dynamics coupled to a linear elasticity system. We finally compare numerical results obtained from the two different approaches.

1. Introduction

Structural topology optimization denotes problems of finding optimal material distributions in a given design domain subject to certain criteria. It has become a standard tool of engineering design, in particular in structural mechanics, see [4] and the literature therein for more details. There are two different problems of importance: (a) the maximization of material stiffness at given mass, and (b) the minimization of mass while keeping a certain stiffness. We consider only the first approach which is known as the minimal compliance problem and is today well understood with respect to its mathematical formulation, see [1] for an overview. Various successful numerical techniques have been proposed, which rely on sensitivity analysis, mathematical programming, homogenization, see [4] for an overview, or more recently on level-set and phase-field methods [2, 32]. The connection to level-set and phase-field methods is best seen using a relation to image processing.

In [9] the analogy between basic concepts of image segmentation and structural topology optimization is clearly illustrated. While level-set methods have become an accepted tool in structural topology optimization, the use of phase-field methods in this field has not yet become popular. There are only a few approaches considered, see [32, 10, 28]. This might be due to the high computational cost of solving the underlying fourth order Cahn-Hilliard equation. We will here consider an approach which reduces the cost by replacing the Cahn-Hilliard equation by a volume conserved second order Allen-Cahn equation. Finally, let us point out that phase field approaches have the advantage that topology changes can easily be handled, see Figures 2 and 3.

The outline of the paper is as follows: In Section 2 we describe the phase field approach. In Section 3 the discretization of the Allen-Cahn and the Cahn-Hilliard equations with elasticity are discussed. In Section 4 numerical results for both approaches are shown and compared with each other, and in Section 5 we draw conclusions.

2. Phase-field approach

We consider a structural topology optimization problem of a statically loaded linear elastic structure. The goal is to compute the material distribution in a given bounded design domain $\Omega \subset \mathbb{R}^d$.

We will describe the material distribution with the help of a phase field variable φ. The phase field φ will take values close to 1 in the void and values close to -1 if material is present. In phase field approaches the interface between material and void is described by a diffuse interfacial layer of a thickness which is proportional to a small length scale parameter ε and at the interface the phase field φ rapidly but smoothly changes its value. We can prescribe a given mass by requiring $\fint_\Omega \varphi = m$ where $m \in (-1, 1)$ and $\fint_\Omega \varphi$ is the mean value of φ. We now assume a linear elastic material with an elasticity tensor $\mathcal{C}_1$ and we model the void with a very small elasticity tensor $\mathcal{C}_2$ where we later choose $\mathcal{C}_2 = \varepsilon^2 \mathcal{C}_1$ but other choices are possible. In the interfacial region we interpolate the elastic properties and set

$$\mathcal{C}(\varphi) = \mathcal{C}_1 + \tfrac{1}{2}(1 + \varphi)(\mathcal{C}_2 - \mathcal{C}_1).$$

We now denote by $\mathbf{u} : \Omega \to \mathbb{R}^d$ the displacement vector and by $\mathcal{E}(\mathbf{u}) := \tfrac{1}{2}(\nabla \mathbf{u} + \nabla \mathbf{u}^t)$ the strain tensor. Assuming that the outer forces are given by a linear functional F on the Sobolev space $H^1(\Omega, \mathbb{R}^d)$ the goal in classical structural topology optimization is to minimize the mean compliance $F(\mathbf{u})$ subject to $\fint_\Omega \varphi(x)dx = m$ and

$$\langle \mathcal{E}(\mathbf{u}), \mathcal{E}(\boldsymbol{\eta}) \rangle_{\mathcal{C}(\varphi)} = F(\boldsymbol{\eta}) \tag{2.1}$$

which has to hold for all $\boldsymbol{\eta} \in H^1(\Omega, \mathbb{R}^d)$ such that $\boldsymbol{\eta} = 0$ on a given non-empty Dirichlet boundary Γ_D. Here we use the notation

$$\langle \mathcal{A}, \mathcal{B} \rangle_{\mathcal{C}} := \int_\Omega \mathcal{A} : \mathcal{C}\mathcal{B}$$

where the :–product of matrices $\mathcal{G}$ and $\mathcal{H}$ is given as $\mathcal{G} : \mathcal{H} := \sum_{i,j=1}^d \mathcal{G}_{ij} \mathcal{H}_{ij}$.

The outer forces F can be given for example by a boundary traction on $\Gamma_F \subset \partial\Omega \setminus \Gamma_D$ and in this case we have

$$F(\boldsymbol{\eta}) = \int_{\Gamma_F} \mathbf{f} \cdot \boldsymbol{\eta} \tag{2.2}$$

where $\mathbf{f} : \Gamma_F \to \mathbb{R}^d$ describes outer forces acting on the structure. The strong formulation of (2.1) with F of the form (2.2) is now given as

$$
\begin{aligned}
-\nabla \cdot [\mathcal{C}(\varphi)\mathcal{E}(\mathbf{u})] &= 0 && \text{in } \Omega \,, \\
\mathbf{u} &= \mathbf{0} && \text{on } \Gamma_D \,, \\
[\mathcal{C}(\varphi)\mathcal{E}(\mathbf{u})] \cdot n &= \mathbf{f} && \text{on } \Gamma_F \,, \\
[\mathcal{C}(\varphi)\mathcal{E}(\mathbf{u})] \cdot n &= \mathbf{0} && \text{on } \partial\Omega \setminus (\Gamma_D \cup F_F) \,,
\end{aligned}
$$

where n is the outer unit normal to $\partial\Omega$. In the above formulation the problem is ill-posed and unwanted checkerboard patterns and mesh dependencies are well-known phenomena, see [27].

A possible regularization is to add a perimeter penalization to the functional which penalizes length for $d = 2$ and area if $d = 3$ for the interface between material and void. This regularization in particular avoids checkerboard patterns if spatial discretization parameters tend to zero, see [18, 23].

In phase field approaches such a penalization can be modeled with the help of a Ginzburg-Landau energy

$$E(\varphi) := \int_\Omega (\tfrac{\gamma\varepsilon}{2} |\nabla\varphi|^2 + \tfrac{\gamma}{\varepsilon} \psi(\varphi)) dx$$

where γ is a parameter related to the interfacial energy density. The potential function $\psi : \mathbb{R} \to \mathbb{R}_0^+ \cup \{\infty\}$ is assumed to have two global minima at the points ± 1. Examples are $\psi(\varphi) = \psi_1(\varphi) := c_1(1 - \varphi^2)^2$ with $c_1 \in \mathbb{R}^+$ or the obstacle potential

$$\psi(\varphi) = \begin{cases} \psi_0(\varphi) & \text{if } |\varphi| \le 1 \,, \\ \infty & \text{if } |\varphi| > 1 \end{cases} \tag{2.3}$$

with e.g. $\psi_0(\varphi) := \tfrac{1}{2}(1 - \varphi^2)$. It is well known that the energy E converges to a scalar multiple of the perimeter functional, see [22].

We now want to solve

$$\min J(\varphi, \mathbf{u}) := E(\varphi) + F(\mathbf{u}) \tag{2.4}$$

subject to (2.1) and $\fint_\Omega \varphi(x)dx = m$. For a given φ we can compute a unique $\mathbf{u}(\varphi)$ with $\mathbf{u}(\varphi) = \mathbf{0}$ on Γ_D which solves (2.1). We can hence consider the reduced

problem

$$\min \hat{J}(\varphi) \quad \text{subject to} \quad \fint_{\Omega} \varphi(x)dx = m \qquad (2.5)$$

with the reduced functional

$$\hat{J}(\varphi) := J(\varphi, \mathbf{u}(\varphi)).$$

In order to compute the first variation of the reduced functional $\hat{J}$ we apply a formal Lagrange approach, see e.g. Hinze et al. [19]. We therefore introduce the adjoint variable $\mathbf{p} : \Omega \to \mathbb{R}^d$ and define the Lagrangian

$$L(\varphi, \mathbf{u}, \mathbf{p}) := E(\varphi) + F(\mathbf{u}) - \langle \mathcal{E}(\mathbf{u}), \mathcal{E}(\mathbf{p}) \rangle_{\mathcal{C}(\varphi)} + F(\mathbf{p}).$$

We now seek stationary states $(\varphi, \mathbf{u}, \mathbf{p})$ of L. If the first variation for $(\varphi, \mathbf{u}, \mathbf{p})$ vanishes we observe that $\mathbf{u}$ and $\mathbf{p}$ both solve (2.1). Assuming $\Gamma_D \neq \emptyset$ we obtain that (2.1) has a unique solution with Dirichlet data on Γ_D and we hence conclude $\mathbf{u} \equiv \mathbf{p}$. Using this we get

$$\tfrac{\delta \hat{J}}{\delta \varphi}(\varphi) = \tfrac{\delta L}{\delta \varphi}(\varphi, \mathbf{u}, \mathbf{p}) = \tfrac{\delta E}{\delta \varphi}(\varphi) - \langle \mathcal{E}(\mathbf{u}), \mathcal{E}(\mathbf{u}) \rangle_{\mathcal{C}'(\varphi)},$$

where $\tfrac{\delta \hat{J}}{\delta \varphi}$, $\tfrac{\delta L}{\delta \varphi}$ and $\tfrac{\delta E}{\delta \varphi}$ denote the first variation with respect to φ and $\mathbf{u}$ solves (2.1).

We now want to use a steepest descent approach in order to find (local) minima of (2.5). We choose a gradient flow dynamics with an artificial time variable and this leads to a pseudo time stepping approach. Given an inner product $\langle ., . \rangle$ the gradient flow for (2.5) with respect to $\langle ., . \rangle$ is given as

$$\begin{aligned} \langle \partial_t \varphi, \zeta \rangle &= -\tfrac{\delta \hat{J}}{\delta \varphi}(\varphi) = -\tfrac{\delta L}{\delta \varphi}(\varphi, \mathbf{u}, \mathbf{p})(\zeta) \\ &= -\int_{\Omega} [\gamma \varepsilon \nabla \varphi \cdot \nabla \zeta + \tfrac{\gamma}{\varepsilon} \psi'(\varphi)\zeta - \mathcal{E}(\mathbf{u}) : \mathcal{C}'(\varphi)\mathcal{E}(\mathbf{u})\zeta] \end{aligned}$$

where $\mathbf{u}$ solves (2.1). Of course the steepest descent method should take the constraint on the total mass given as $\fint_{\Omega} \varphi(x) = m$ into account. Furthermore, the steepest descent direction is given by the gradient and the gradient of course depends on the inner product chosen. As inner product we either choose the L^2–inner product which results in an Allen-Cahn type dynamics or the mass conserving H^{-1}–inner product leading to a modified Cahn-Hilliard problem.

In the following we briefly discuss how we obtain the Allen-Cahn dynamics and a modified Cahn-Hilliard equation as gradient flows. For further details we refer to [29] and [5].

We first formulate the problem in the case that $\langle ., . \rangle$ is given by a scaled L^2–inner product $(., .)$ leading to an Allen-Cahn type dynamics, where also the mass constraint $\fint_{\Omega} \varphi = m$ has to be enforced. Using the obstacle potential (2.3) we obtain on an arbitrary time interval $(0, T)$ (see [6] for further details):

($\mathbf{P}_1$) *Find $\varphi \in H^1(\Omega_T)$ and $\mathbf{u} \in L^\infty(0,T; H^1(\Omega, \mathbb{R}^d))$ such that*

$$\fint_\Omega \varphi(x,t)dx = m, \varphi(.,0) = \varphi_0, |\varphi| \leq 1 \ a.e. \ in \ \Omega_T, \mathbf{u} = 0 \ a.e. \ on \ \Gamma_D \times (0,T),$$

$$(\varepsilon\partial_t\varphi + \tfrac{\gamma}{\varepsilon}\psi_0'(\varphi), \chi - \varphi) + \gamma\varepsilon(\nabla\varphi, \nabla(\chi - \varphi)) \geq \tfrac{1}{2}\langle \mathcal{E}(\mathbf{u}), \mathcal{E}(\mathbf{u})(\chi - \varphi)\rangle_{\mathcal{C}_2 - \mathcal{C}_1},$$

$$\langle \mathcal{E}(\mathbf{u}), \mathcal{E}(\boldsymbol{\eta})\rangle_{\mathcal{C}(\varphi)} = F(\boldsymbol{\eta})$$

*which has to hold for almost all t and all $\chi \in H^1(\Omega)$ with $|\chi| \leq 1$ and $\fint_\Omega \chi = m$
and all $\boldsymbol{\eta} \in H^1(\Omega, \mathbb{R}^d)$ such that $\boldsymbol{\eta} = 0$ on the Dirichlet boundary Γ_D.*

We now discuss the mass conserving H^{-1}–gradient flow which leads to the Cahn-Hilliard type dynamics. For functions v_1, v_2 with mean value zero we define the inner product

$$(v_1, v_2)_{-1} := \int_\Omega \nabla(-\Delta)^{-1}v_1 \cdot \nabla(-\Delta)^{-1}v_2$$

where $y = (-\Delta)^{-1}v$ is the weak solution of $-\Delta y = v$ in Ω with $\fint_\Omega y = 0$ and
$\frac{\partial y}{\partial n} = 0$ on $\partial\Omega$. The H^{-1}–gradient flow

$$(\partial_t\varphi, \chi)_{-1} = -\tfrac{\delta L}{\delta\varphi}(\varphi, \mathbf{u}, \mathbf{p})(\chi)$$

can now be rewritten by introducing the chemical potential $w = -(-\Delta)^{-1}\partial_t\varphi + \overline{w}$ where $\overline{w}$ is an appropriate constant. Considering the smooth potential $\psi = \psi_1$ and a variable diffusivity B, we obtain the following problem which is a modified Cahn-Hilliard equation, see also [14, 20].

($\mathbf{P}_2$) *Find sufficiently regular $(\varphi, w, \mathbf{u})$ such that*

$$\varphi(.,0) = \varphi_0, |\varphi| \leq 1 \ a.e., \ \mathbf{u} = \mathbf{0} \ a.e. \ on \ \Gamma_D \times (0,T) \ and$$

$$\partial_t\varphi = \nabla \cdot (B(\varphi)\nabla w) \ in \ the \ distributional \ sense, \tag{2.6}$$

$$\tfrac{\partial w}{\partial n} = 0, \tfrac{\partial\varphi}{\partial n} = 0 \ on \ \partial\Omega \times (0,T),$$

$$w = -\gamma\varepsilon\Delta\varphi + \tfrac{\gamma}{\varepsilon}\psi_1'(\varphi) - \mathcal{E}(\mathbf{u}) : \mathcal{C}'(\varphi)\mathcal{E}(\mathbf{u}) \ in \ the \ distributional \ sense$$

together with (2.1).

Strictly speaking we obtain ($\mathbf{P}_2$) as the gradient flow of $(.,.)_{-1}$ only in the case that the mobility function B in (2.6) is equal to one. We refer to Taylor and Cahn [29] who discuss how the definition of $(.,.)_{-1}$ has to be modified for a variable mobility. With this modification we obtain (2.6) also for a variable mobility. We also remark that (2.6) together with the Neumann boundary conditions on w imply that the mass $\int_\Omega \varphi$ is preserved. For further information on elastically modified Cahn-Hilliard models we refer to the overview [15].

Stationary states of ($\mathbf{P}_1$) and ($\mathbf{P}_2$) respectively fulfil the first order necessary conditions for (2.4). In the following section we describe how we numerically solve ($\mathbf{P}_1$) and ($\mathbf{P}_2$) and in Section 4 we will compare numerical results of ($\mathbf{P}_1$) and ($\mathbf{P}_2$).

3. Discretization

In this section we present finite element approximations of $(\mathbf{P}_1)$ and $(\mathbf{P}_2)$.

3.1. Notation

For simplicity we assume that Ω is a polyhedral domain. Let $\mathcal{T}_h$ be a regular triangulation of Ω into disjoint open simplices, i.e. $\Omega = \cup_{T \in \mathcal{T}_h} \overline{T}$. Furthermore, we define $h := \max_{T \in \mathcal{T}_h} \{\text{diam } T\}$ the maximal element size of $\mathcal{T}_h$ and we set $\mathcal{J}$ to be the set of nodes of $\mathcal{T}_h$ and $\{p_j\}_{j \in \mathcal{J}}$ to be the coordinates of these nodes. Associated with $\mathcal{T}_h$ is the piecewise linear finite element space

$$S_h := \left\{ \eta \in C^0(\overline{\Omega}) \,\Big|\, \eta\big|_T \in P_1(T) \ \forall \ T \in \mathcal{T}_h \right\} \subset H^1(\Omega),$$

where we denote by $P_1(T)$ the set of all affine linear functions on T. Furthermore, we denote the standard nodal basis functions of S_h by χ_j for all $j \in \mathcal{J}$. Then φ_j for $j = 1, \ldots \mathcal{J}$ denote the coefficients of the basis representation of φ_h in S_h which is given by $\varphi_h = \sum_{j \in \mathcal{J}} \varphi_j \chi_j$.

In order to derive a discretization of $(\mathbf{P}_1)$ we define

$$\mathcal{K}_h^m := \{\eta \in S_h \,|\, |\eta(x)| \leq 1 \text{ for all } x \in \Omega, \fint_\Omega \eta dx = m\}.$$

We introduce also the lumped mass scalar product $(f, g)_h = \int_\Omega I_h(fg)$ instead of (f, g), where $I_h : C^0(\overline{\Omega}) \to S_h$ is the standard interpolation operator such that $(I_h f)(p_j) = f(p_j)$ for all nodes $j \in \mathcal{J}$. In addition, we employ a quadrature formula $\langle \mathcal{A}, \mathcal{B} \rangle_{\mathcal{C}}^h$ in place of $\langle \mathcal{A}, \mathcal{B} \rangle_{\mathcal{C}}$, with the property that $\langle \mathcal{A}, \mathcal{B} \rangle_{\mathcal{C}}^h = \langle \mathcal{A}, \mathcal{B} \rangle_{\mathcal{C}}$ for piecewise affine linear integrands $\mathcal{A} : \mathcal{C}\mathcal{B}$.

3.2. Finite element approximation of the Allen-Cahn approach with mass conservation and obstacle potential

Taking a fixed time step $\tau = t_n - t_{n-1}$ we obtain the following finite element approximation of $(\mathbf{P}_1)$:

$(\mathbf{P}_1^h)$ *Given* $\varphi_h^{n-1} \in \mathcal{K}_h^m$ *find* $(\varphi_h^n, \mathbf{u}_h^n) \in \mathcal{K}_h^m \times (S_h)^d$ *such that*

$$\mathbf{u}_h^n = 0 \text{ on } \mathbf{\Gamma}_D,$$

$$\langle \mathcal{E}(\mathbf{u}_h^n), \mathcal{E}(\boldsymbol{\eta}) \rangle_{\mathcal{C}(\varphi_h^{n-1})}^h = F(\boldsymbol{\eta}) \ \forall \ \boldsymbol{\eta} \in (S_h)^d \text{ with } \boldsymbol{\eta} = 0 \text{ on } \Gamma_D, \tag{3.1}$$

$$\left(\tfrac{\varepsilon}{\tau}(\varphi_h^n - \varphi_h^{n-1}) - \tfrac{\gamma}{\varepsilon}\varphi_h^n, \chi - \varphi_h^n\right)_h + \gamma\varepsilon(\nabla\varphi_h^n, \nabla(\chi - \varphi_h^n))$$
$$\geq \tfrac{1}{2}\langle \mathcal{E}(\mathbf{u}_h^n), \mathcal{E}(\mathbf{u}_h^n)(\chi - \varphi_h^n) \rangle_{\mathcal{C}_2 - \mathcal{C}_1}^h \ \ \forall \chi \in \mathcal{K}_h^m. \tag{3.2}$$

As (3.1) is independent of φ_h^n we use a preconditioned conjugate gradient solver to compute $\mathbf{u}_h^n$ from this equation, see also [17, 16]. Due to the use of piecewise linear finite elements and mass lumping the reformulation of (3.2) with Lagrange multipliers $\mu_h \in S_h$ and $\lambda \in \mathbb{R}$ can be stated as follows, see [6]:

Given $(\varphi_h^{n-1}, \mathbf{u}_h^n) \in \mathcal{K}_h^m \times (S_h)^d$, *find* $\varphi_h^n \in \mathcal{K}_h^m$, $\mu_h \in S_h$ *and* $\lambda \in \mathbb{R}$ *such that*

$$(\tfrac{\varepsilon^2}{\tau} - \gamma)(\varphi_h^n, \chi)_h + \gamma\varepsilon^2(\nabla\varphi_h^n, \nabla\chi) + (\mu_h, \chi)_h - \lambda(1, \chi)$$

$$= \tfrac{\varepsilon^2}{\tau}(\varphi_h^{n-1}, \chi)_h + \tfrac{\varepsilon}{2}\langle\mathcal{E}(\mathbf{u}_h^n), \mathcal{E}(\mathbf{u}_h^n)\chi\rangle_{\mathcal{C}_2-\mathcal{C}_1}^h \ \forall \chi \in S_h, \quad (3.3)$$

$$\fint_\Omega \varphi_h^n = m, \tag{3.4}$$

$$(\mu_j)_- \geq 0, \ (\mu_j)_+ \geq 0, \ |\varphi_j| \leq 1, \tag{3.5}$$

$$(\varphi_j + 1)(\mu_j)_- = (\varphi_j - 1)(\mu_j)_+ = 0 \ \forall \ j \in \mathcal{J}, \tag{3.6}$$

where $(.)_+$ and $(.)_-$ are the positive and negative parts of a quantity in the brackets.

To solve (3.3)-(3.6) we apply the PDAS-method presented in [6], yielding the following algorithm:

Primal-Dual Active Set Algorithm (PDAS):

0. *Set $k = 0$ and initialize $\mathcal{A}_0^\pm$.*
1. *Define $\mathcal{I}_k = \mathcal{J} \setminus (\mathcal{A}_k^+ \cup \mathcal{A}_k^-)$.*
   Set $\varphi_j^k = \pm 1$ for $j \in \mathcal{A}_k^\pm$ and $\mu_j^k = 0$ for $j \in \mathcal{I}_k$.
2. *Solve the discretized PDE (3.3) with the non-local constraint (3.4) to obtain φ_j^k for $j \in \mathcal{I}_k$ and $\lambda^k \in \mathbb{R}$.*
3. *Determine μ_j^k for $j \in \mathcal{A}_k^\pm$ using (3.3).*
4. *Set $\mathcal{A}_{k+1}^+ := \{j \in \mathcal{J} : \varphi_j^k + \tfrac{\mu_j^k}{c} > 1\}$, $\mathcal{A}_{k+1}^- := \{j \in \mathcal{J} : \varphi_j^k + \tfrac{\mu_j^k}{c} < -1\}$.*
5. *If $\mathcal{A}_{k+1}^\pm = \mathcal{A}_k^\pm$ stop, otherwise set $k = k + 1$ and goto 1.*

Remark 3.1. We solve the system arising from Step 2 using MINRES, see [8].

The Allen-Cahn variational inequality with volume constraint is implemented using the adaptive finite element toolbox Alberta 1.2 [26].

3.3. Finite element approximation of the Cahn-Hilliard approach with smooth potential

For the case of a fixed time step $\tau = t_n - t_{n-1}$ we obtain the following finite element approximation of $(\mathbf{P}_2)$:

$(\mathbf{P}_2^h)$ *Given $\varphi_h^{n-1} \in S_h$ find $(\varphi_h^n, w_h^n, \mathbf{u}_h^n) \in S_h \times S_h \times (S_h)^d$ such that*

$$\mathbf{u}_h^n = 0 \ on \ \boldsymbol{\Gamma}_D, \tag{3.7}$$

$$\langle\mathcal{E}(\mathbf{u}_h^n), \mathcal{E}(\boldsymbol{\eta})\rangle_{\mathcal{C}(\varphi_h^{n-1})}^h = F(\boldsymbol{\eta}) \ \forall \ \boldsymbol{\eta} \in (S_h)^d \ with \ \boldsymbol{\eta} = 0 \ on \ \boldsymbol{\Gamma}_D, \tag{3.8}$$

$$(\tfrac{\varepsilon}{\tau}(\varphi_h^n - \varphi_h^{n-1}), \chi)_h + (B(\varphi_h^{n-1})\nabla w_h^n, \nabla\chi)_h = 0 \ \forall \ \chi \in S_h, \tag{3.9}$$

$$(w_h^n, \chi)_h = \gamma\epsilon(\nabla\varphi_h^n, \nabla\chi)_h + \tfrac{\gamma}{\epsilon}(\psi_1'(\varphi_h^{n-1}) + \psi_1''(\varphi_h^{n-1})(\varphi_h^n - \varphi_h^{n-1}), \chi)_h$$
$$- \tfrac{1}{2}\langle\mathcal{E}(\mathbf{u}_h^n), \mathcal{E}(\mathbf{u}_h^n)\chi\rangle_{\mathcal{C}_2-\mathcal{C}_1}^h \ \ \forall\chi \in S_h, \tag{3.10}$$

where $B(\varphi) = \tfrac{9}{4}(1 - \varphi^2)^2$.

We solve equation (3.8) as in $(\mathbf{P}_1)$. Equations (3.9) and (3.10) on the other hand, define a system of two discretized second order equations for φ_h^n and the
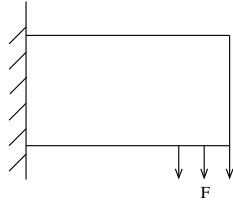
FIGURE 1. The design domain for a cantilever beam

chemical potential w_h^n. The derivative of the double well potential was linearized as $\psi_1'(\varphi_h^n) \approx \psi_1'(\varphi_h^{n-1}) + \psi_1''(\varphi_h^{n-1})(\varphi_h^n - \varphi_h^{n-1})$ with $\psi_1'(\varphi) = \frac{9}{8}(1-\varphi^2)^2$, see (3.10). The resulting linear system is solved using BiCGStab, see [25, 31] for details.

The Cahn-Hilliard equation is implemented using the adaptive finite element toolbox AMDiS [31].

4. Numerics

In this section we present some numerical results for both the Allen-Cahn and the Cahn-Hilliard approach.

Since the interfacial thickness in both approaches is proportional to ε we need to choose $h \ll \varepsilon$ in order to resolve the interfacial layer (see [11, 12] for details). Away from the interface h can be chosen larger and hence adaptivity in space can heavily speed up computations. We use the same mesh refinement strategy as in Barrett, Nürnberg and Styles [3], i.e. a fine mesh is constructed where $|\varphi_h^{n-1}| < 1$ with a coarser mesh present in the bulk regions $\varphi_h^{n-1} = \pm 1$. We set the interfacial parameters $\varepsilon = \frac{1}{16\pi}$ and $\gamma = 1$ and we take the minimal diameter of an element $h_{min} = 7.81 \times 10^{-3}$ and the maximal diameter $h_{max} = 6.25 \cdot 10^{-2}$. The time step is chosen as $\tau = 6.25 \cdot 10^{-6}$ for the Allen-Cahn approach. In the Cahn-Hilliard case an adaptive time step is used.

We use a cantilever beam geometry, see Figure 1, where we pose Dirichlet boundary conditions on the left boundary Γ_D and a vertical force is acting at the bottom of its free vertical edge. We take $\Omega = (-1, 1) \times (0, 1)$, and hence $\Gamma_D = \{(-1, y) \in \mathbb{R}^2 : y \in [0, 1]\}$. The force F is acting on $\Gamma_F := \{(x, 0) \in \mathbb{R}^2 : x \in [0.75, 1]\}$ and is defined by $\mathbf{f}(x) = (0, 250)^t$ for $x \in \Gamma_F$. In our computations we use an isotropic elasticity tensor $\mathcal{C}_1$ of the form $\mathcal{C}_1 \mathcal{E} = 2\mu_1 \mathcal{E} + \lambda_1 (tr\mathcal{E})I$ with the Lamé constants $\lambda_1 = \mu_1 = 5000$ and choose $\mathcal{C}_2 = \varepsilon^2 \mathcal{C}_1$ in the void. We initialize the order parameter φ with random values between -0.1 and 0.1 for the Allen-Cahn approach and -0.2 and 0.2 for the Cahn-Hilliard approach. In both cases the random field ensures that we approximately have the same proportion of material and void, i.e. $m \approx 0$.

Figure 2 shows the results obtained using the Allen-Cahn variational inequality with volume constraint, where the state at $t = 0.160$ appears to be a numerical steady state.
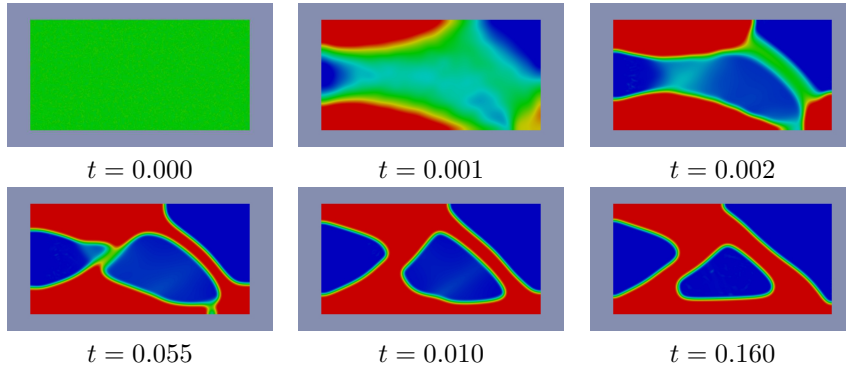
FIGURE 2. Allen-Cahn results for the cantilever beam computation at various times; material in red and void in blue

Figure 3 shows the results obtained using the Cahn-Hilliard equation with a variable mobility. Again the state at $t = 0.168$ appears to be a numerical steady state.
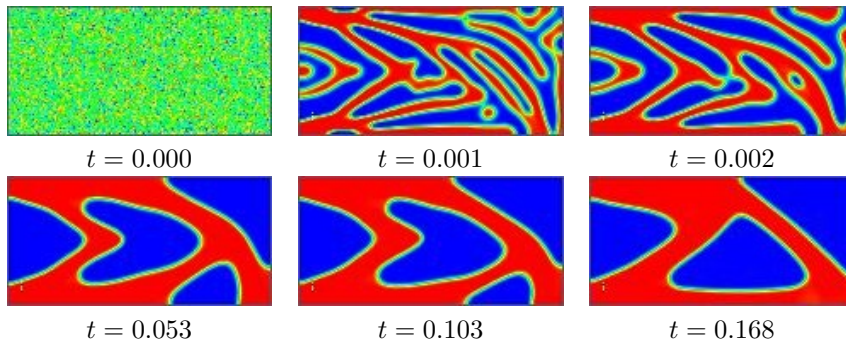

FIGURE 3. Cahn-Hilliard results for the cantilever beam computation at various times; material in red and void in blue

A comparison of both simulations gives two results: First the obtained optimal shape is almost the same, and second the evolution towards this shape is very different. Within the Allen-Cahn approach the final structure evolved directly from the random initial state within the same spatial scale. Also "new material" can be formed during the evolution in regions which previously have been occupied by void material. Within the Cahn-Hilliard approach such forming of "new material" was never observed. Instead the evolution always follows a coarsening process from fine scale structures, as a result of the spinodal decomposition in the early evolution, to coarser scales.

5. Conclusions

The use of phase-field methods in structural topology optimization has been limited due to high computational cost, associated with solving the underlying fourth order Cahn-Hilliard equation. We have demonstrated on a simple example that a volume conserved Allen-Cahn equation can be used instead, which reduces the computational cost and thus makes the phase-field approach more efficient. We also point out that an obstacle potential together with the primal-dual active set approach allows us to compute for the phase field only in the interfacial region which reduces the total size of the problem, see also [5, 6]. We also mention that phase field approaches can be generalized for multimaterial structural topology optimization, see [32] for the Cahn-Hilliard case and [7] for the Allen-Cahn case.

We further want to point out, that the use of phase-field methods might also allow structural topology optimization to be extended to other fields besides structural mechanics. Due to the flexibility of the phase-field approach it can easily be coupled with other fields, such as flow, temperature or concentration fields. In [24, 21, 30, 13] a method is described which allows it to solve general partial differential equations with general boundary conditions in evolving geometries, which are implicitly described using a phase-field function. Allowing the phase-field function to evolve in order to minimize an objective function, which depends on the variables of the partial differential equation to be solved, will lead to new structural topology optimization problems.

References

[1] G. Allaire, *Optimization by the Homogenization Method.* Springer, Berlin 2002.

[2] G. Allaire, F. Jouve, A.-M. Toader, *Structural optimization using sensitivity analysis and a level-set method.* J. Comput. Phys. **194** (2004), 363-393.

[3] J.W. Barrett, R. Nürnberg, V. Styles, *Finite element approximation of a phase field model for void electromigration.* SIAM J. Numer. Anal. **46** (2004), 738-772.

[4] M.P. Bendsoe, O. Sigmund, *Topology Optimization.* Springer, Berlin 2003.

[5] L. Blank, M. Butz, H. Garcke, *Solving the Cahn-Hilliard variational inequality with a semi-smooth Newton method.* DFG priority program 1253 "Optimization with PDEs", Preprint No. 1253-09-02.

[6] L. Blank, H. Garcke, L. Sarbu, V. Styles, *Primal-dual active set methods for Allen-Cahn variational inequalities with non-local constraints.* DFG priority program 1253 "Optimization with PDEs", Preprint No. 1253-09-01.

[7] L. Blank, H. Garcke, L. Sarbu, V. Styles, *Non-local Allen-Cahn systems: Analysis and primal dual active set methods.* In preparation.

[8] L. Blank, L. Sarbu, M. Stoll, *Preconditioning for Allen-Cahn variational inequalities with non-local constraints.* In preparation.

[9] B. Bourdin, A. Chambolle, *Design-dependent loads in topology optimization.* ESIAM Control Optim. Calc. Var. **9** (2003), 19-48.

[10] M. Burger, R. Stainko, *Phase-field relaxation of topology optimization with local stress constraints.* SIAM J. Control Optim. **45** (2006), 1447-1466.

[11] C.M. Elliott, *Approximation of curvature dependent interface motion.* State of the art in Numerical Analysis, IMA Conference Proceedings **63**, Clarendon Press, Oxford, 1997, 407-440.

[12] C.M. Elliott, V. Styles, *Computations of bi-directional grain boundary dynamics in thin films.* J. Comput. Phys. **187** (2003) 524-543.

[13] C.M. Elliott, B. Stinner, V. Styles, R. Welford, *Numerical computation of advection and diffusion on evolving diffuse interfaces.* IMA J. Num. Anal. (2009), (to appear).

[14] H. Garcke, *On Cahn-Hilliard systems with elasticity.* Proc. Roy. Soc. Edinburgh Sect. A **133** (2003), no. 2, 307-331.

[15] H. Garcke, *Mechanical effects in the Cahn-Hilliard model: A review on mathematical results.* In "Mathematical Methods and Models in phase transitions", ed.: Alain Miranville, Nova Science Publ. (2005), 43-77.

[16] H. Garcke, R. Nürnberg, V. Styles, *Stress and diffusion induced interface motion: Modelling and numerical simulations.* European Journal of Applied Math. **18** (2007), 631-657.

[17] H. Garcke, U. Weikard, *Numerical approximation of the Cahn-Larché equation.* Numer. Math. **100** (2005) 639-662.

[18] R.B. Haber, C.S. Jog, M.P. Bendsøe, *A new approach to variable topology shape design using a constraint on perimeter.* Struct. Multidisc. Optim. **11** (1996), 1-12.

[19] M. Hinze, R. Pinnau, M. Ulbrich, S. Ulbrich *Optimization with PDE Constraints.* Mathematical Modelling: Theory and Applications **23**, Springer (2008).

[20] F.C. Larché, J.W. Cahn, *The effect of self-stress on diffusion in solids*, Acta Metall. **30** (1982) 1835-1845.

[21] X. Li, J. Lowengrub, A. Rätz, A. Voigt, *Solving PDEs in complex geometries- a diffuse domain approach.* Comm. Math. Sci. **7** (2009), 81-107.

[22] L. Modica, *The gradient theory of phase transitions and the minimal interface criterion.* Arch. Rat. Mech. Anal. **98** (1987), 123-142.

[23] J. Petersson, *Some convergence results in perimeter-controlled topology optimization.* Computer Meth. Appl. Mech. Eng. **171** (1999), 123-140.

[24] A. Rätz, A. Voigt, *PDEs on surfaces - a diffuse interface approach.* Comm. Math. Sci. **4** (2006), 575-590.

[25] A. Rätz, A. Ribalta, A. Voigt, *Surface evolution of elastically stressed films under deposition by a diffuse interface model.* J. Comput. Phys. **214** (2006) 187-208.

[26] A. Schmidt, K.G. Siebert, *Design of adaptive finite element software. The finite element toolbox ALBERTA*, Lecture Notes in Computational Science and Engineering 42. Springer-Verlag, Berlin, 2005.

[27] O. Sigmund, J. Petersson, *Numerical instabilities in topology optimization: A survey on procedures dealing with checkerboards, mesh-dependencies and local minima.* Struct. Multidisc. Optim. **16** (1998), 68-75.

[28] A. Takezawa, S. Nishiwaki, M. Kitamura, *Shape and topology optimization based on the phase field method and sensitivity analysis.* Journal of Computational Physics **229** (7) (2010), 2697-2718.

[29] J.E. Taylor, J.W. Cahn, *Linking anisotropic sharp and diffuse surface motion laws via gradient flows.* J. Statist. Phys. **77** (1994), no.1-2, 183-197.

[30] K.E. Teigen, X. Li, J. Lowengrub, F. Wang, A. Voigt, *A diffuse-interface approach for modeling transport, diffusion and adsorption/desorption of material quantities on a deformable interface.* Comm. Math. Sci. **7** (2009), 1009-1037.

[31] S. Vey, A. Voigt, *AMDiS - adaptive multidimensional simulations.* Comput. Vis. Sci. **10** (2007) 57-67.

[32] M.Y. Wang, S.W. Zhou, *Phase field: A variational method for structural topology optimization.* Comput. Model. Eng. Sci. **6** (2004) 547-566.

Luise Blank
NWF I - Mathematik
Universität Regensburg
93040 Regensburg, Germany
e-mail: `luise.blank@mathematik.uni-regensburg.de`

Harald Garcke
NWF I - Mathematik
Universität Regensburg
93040 Regensburg, Germany
e-mail: `harald.garcke@mathematik.uni-regensburg.de`

Lavinia Sarbu
Department of Mathematics
University of Sussex
Brighton BN1 9RF, UK
e-mail: `ls99@sussex.ac.uk`

Tarin Srisupattarawanit
Institut für Wissenschaftliches Rechnen
TU Dresden
01062 Dresden, Germany
e-mail: `tarin.srisupattarawanit@tu-dresden.de`

Vanessa Styles
Department of Mathematics
University of Sussex
Brighton BN1 9RF, UK
e-mail: `v.styles@sussex.ac.uk`

Axel Voigt
Institut für Wissenschaftliches Rechnen
TU Dresden
01062 Dresden, Germany
e-mail: `axel.voigt@tu-dresden.de`